Available online at www.sciencedirect.com
ScienceDirect
Journal of Photochemistry and Photobiology A: Chemistry 195 (2008) 205–214
Journal of Photochemistry and Photobiology A:Chemistry
www.elsevier.com/locate/jphotochem

Pilot plant scale reactive dyes degradation by solar photo-Fenton and biological processes

Julia García-Montaño [a,*], Leonidas Pérez-Estrada [b], Isabel Oller [b], Manuel I. Maldonado [b], Francesc Torrades [c], José Peral [a]

[a] *Departament de Química, Edifici Cn, Universitat Autònoma de Barcelona, 08193 Bellaterra (Barcelona), Spain*
[b] *Plataforma Solar de Almería-CIEMAT, Carretera Senés km 4, 04200 Tabernas (Almería), Spain*
[c] *Departament d'Enginyeria Química, ETSEIA de Terrassa (UPC), C/Colom 11, 08222 Terrassa (Barcelona), Spain*

Received 5 February 2007; received in revised form 17 July 2007; accepted 5 October 2007
Available online 16 October 2007

Abstract

Solar photo-Fenton reactions as a stand-alone process and as a pre-treatment of an aerobic biological treatment for Procion Red H-E7B and Cibacron Red FN-R reactive dyes degradation have been carried out at pilot plant scale. Photo-Fenton oxidation was conducted using a Compound Parabolic Collector (CPC) solar photo-reactor and the biological treatment was carried out with an Immobilised Biomass Reactor (IBR). Artificial light photo-Fenton experiments carried out at laboratory scale have been taken as starting point. When applying photo-Fenton reaction as a single process, 10 mg L^{-1} Fe (II) and 250 mg L^{-1} H_2O_2 for 250 mg L^{-1} Procion Red H-E7B treatment, and 20 mg L^{-1} Fe (II) and 500 mg L^{-1} H_2O_2 for 250 mg L^{-1} Cibacron Red FN-R treatment closely reproduced the laboratory mineralisation results, with 82 and 86% Dissolved Organic Carbon (DOC) removal, respectively. Nevertheless, the use of sunlight with the CPC photo-reactor increased the degradation rates allowing the reduction of Fe (II) concentration from 10 to 2 mg L^{-1} (Procion Red H-E7B) and from 20 to 5 mg L^{-1} (Cibacron Red FN-R) without yield loses. Carboxylic acids, SO_4^{2-}, NH_4^+ and NO_3^- generation was monitored along with dye mineralisation. Finally, in the combined photo-Fenton/biological system, reagents doses of 5 mg L^{-1} Fe (II) and 225 mg L^{-1} H_2O_2 for Cibacron Red FN-R and 2 mg L^{-1} Fe (II) and 65 mg L^{-1} H_2O_2 for Procion Red H-E7B were enough to generate biodegradable solutions that could be fed to the IBR, even improving bench-scale results.

Keywords: Immobilised Biomass Reactor; Photo-Fenton; Pilot plant; Reactive dyes; Sunlight

1. Introduction

Textile industry consumes large volumes of water in dyeing and finishing operations. In textile dyebaths, the degree of fixation of dyes is never complete resulting in dye-containing effluents [1]. The release of such coloured wastewaters into the environment is a dramatic source of aesthetic pollution, eutrophication and perturbations in aquatic life. Due to their chemical stability, most manufactured dyes are not amenable to common chemical or biological treatments. The increased public concern and the stringent international environmental standards (ISO 14001, November 2004) have prompted the need to develop novel treatment methods for converting organic contaminants, such as dyestuffs, into harmless final products.

Advanced Oxidation Processes (AOPs) are powerful technologies for the remediation of wastewaters containing recalcitrant organic pollutants [2]. Although AOPs include different reacting systems, their mechanisms are basically characterised by the in situ generation of highly reactive and non-selective hydroxyl radicals ($HO^\bullet$, $E^\circ = 2.8$ V versus NHE), species that are able to oxidise and mineralise almost all organic compounds to CO_2 and inorganic ions. Among the available AOPs, Fenton and photo-Fenton processes are of special interest because they make possible the achievement of high reaction yields with a low treatment cost [3]. In dark Fenton reaction (Eq. (1), H_2O ligands on the iron coordination sphere are henceforth omitted), hydroxyl radicals are generated by the interaction between H_2O_2 and ferrous salts. The generated Fe (III) can be reduced by reaction with the exceeding H_2O_2 to form again ferrous ion in a catalytic mechanism (Eqs. (2) and (3)) [4].

$$Fe(II) + H_2O_2 \rightarrow Fe(III) + HO^\bullet + HO^- \quad (1)$$

* Corresponding author. Tel.: +34 93 581 2164; fax: +34 93 581 2920.
E-mail address: julia@klingon.uab.es (J. García-Montaño).

1010-6030/$ – see front matter © 2007 Elsevier B.V. All rights reserved.
doi:10.1016/j.jphotochem.2007.10.004

$$Fe(III) + H_2O_2 \rightarrow HO_2^{\bullet} + Fe(II) + H^+ \quad (2)$$

$$Fe(III) + HO_2^{\bullet} \rightarrow Fe(II) + O_2 + H^+ \quad (3)$$

Radiation can play different roles that lead to an improvement of the reaction yields. It drives photo-Fenton reaction by means of ferric aquo-complexes photolysis, producing extra $HO^{\bullet}$, and the recovery of the Fe (II) needed in Fenton reaction (Eq. (4), being [Fe (III) HO]$^{2+}$ the dominant ferric species in solution at pH 2–3) [5]. The irradiated process may also involve photolysis of an Fe (III)–H_2O_2 complex to form high-valence Fe intermediates, which can directly oxidise organic matter [6]. Moreover, it can drive ligand to metal charge transfer in the potentially photolabile complexes formed by Fe (III) and organic compounds (Eq. (5)), a process that has been well proven for the complexes formed between Fe (III) and the carboxylic acid moiety [7]. In the combined Fenton/photo-Fenton system iron acts as a catalyst and the rate-limiting step is the regeneration of ferrous ion.

$$[Fe\ (III)\ HO]^{2+} \xrightarrow{h\upsilon} Fe\ (II) + HO^{\bullet} \quad (4)$$

$$[Fe\ (III)\ L]^{2+} \xrightarrow{h\upsilon} Fe\ (II) + L^{\bullet} \quad (L = \text{organic ligand}) \quad (5)$$

Since photo-assisted processes may require radiations from UV up to visible (~550 nm) light [7,8], they can be potentially driven under solar irradiation offering additional economic and environmental advantages. Another important improvement for the reduction of economic and environmental impacts is the possibility of using such AOP as a pre-treatment of a conventional biological treatment, a suitable approach for the removal of non-biodegradable compounds in water. Lower amounts of chemicals and energy should then be supplied to achieve a fully biodegradable intermediate solution [9–11].

The bench-scale artificial light assisted photo-Fenton process alone and as a pre-treatment of an aerobic biological process for the degradation of two textile reactive dyes (Procion Red H-E7B, a homo-bireactive dye with two monochlorotriazine groups, and Cibacron Red FN-R, a hetero-bireactive dye with vinylsulphone and fluorotriazine reactive groups) has been previously reported by our group [10,12,13]. Taking into consideration such experiments, the scaling-up from laboratory to pilot plant is performed in this work. Photo-Fenton experiments are conducted at the Plataforma Solar de Almería (PSA, Spain) in a Compound Parabolic Collector (CPC) photo-reactor under solar irradiation. Initially, a single photo-Fenton process with different Fe (II) concentrations is applied in order to mineralise the reactive dye. Dye disappearance, Dissolved Organic Carbon (DOC), H_2O_2 and Fe evolution, carboxylic acids generation and inorganic heteroatoms release are studied as a function of irradiation time. Additionally, biodegradability enhancement as a function of H_2O_2 consumed is assessed for the possibility of a combined chemical/aerobic biological process. In a second part, the photo-Fenton process precedes an aerobic biological treatment carried out in an Immobilised Biomass Reactor (IBR). The minimum H_2O_2 dosage needed to generate completely biodegradable photo-treated solutions is quantified. Finally, the viability of the photo-Fenton process (alone or coupled to a secondary bio-treatment step) for the treatment of the above reactive dyes at pilot plant scale is discussed.

2. Experimental

2.1. Synthetic dye solutions

Commercial Procion Red H-E7B (C.I. Reactive Red 141, $C_{52}H_{34}O_{26}S_8Cl_2N_{14}$, DyStar) and Cibacron Red FN-R (C.I. Reactive Red 238, $C_{29}H_{19}O_{13}S_4ClFN_7$, CIBA) reactive dyes were used as received to prepare synthetic dye solutions. Their purity degree was unknown. The molecular formula of Procion Red H-E7B is shown in Fig. 1. Cibacron Red FN-R chemical structure was not disclosed by the supplier. The initial concentration of the commercial dyes was 250 mg L^{-1}. In order to convert them into the chemical form normally found in industrial effluents, the solutions were hydrolysed by adjusting the pH to 10.6 and heating to a constant temperature of 80 °C for 6 h and 60 °C for 1 h for Procion Red H-E7B and Cibacron Red FN-R, respectively. Some analytical parameters of the hydrolysed dye solutions were: DOC = 40 ± 1 and 69 ± 2 mg L^{-1} C (n = 3, α = 0.05); Chemical Oxygen Demand (COD) = 108 and 200 mg L^{-1} O_2; BOD_5/COD ratio = 0.10 and 0.02.

2.2. Chemicals

All chemicals used throughout this study were of the highest commercially available grade. Iron sulphate ($FeSO_4 \cdot 7H_2O$, Panreac) and hydrogen peroxide (H_2O_2 30% (w/v), Panreac) were used as received. Sulphuric acid and sodium hydroxide solutions were used for pH adjustments. Pilot plant water was obtained from the PSA distillation plant (conductivity <10 μS cm^{-1}, SO_4^{2-} = 0.5 mg L^{-1}, Cl^- = 0.7–0.8 mg L^{-1},

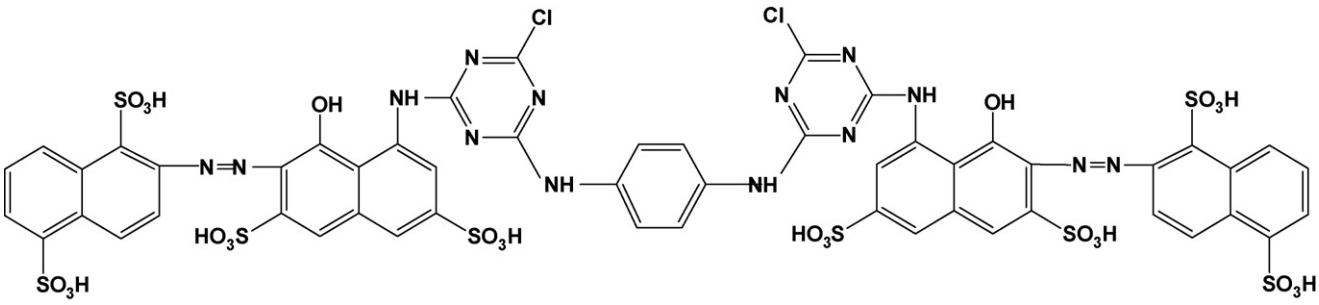

Fig. 1. Chemical structure of Procion Red H-E7B.

organic carbon <0.5 mg L^{-1} C). Ultra pure distilled-deionised water from a Milli-Q (Millipore Co.) system was employed to prepare all the reagent solutions.

2.3. Sample analysis

DOC was determined with a TOC Shimadzu 5050A analyser provided with an ASI-5000A Shimadzu Autosampler. COD was assessed by the closed reflux colorimetric method [14] with a Spectroquant® kit (10–150 mg L^{-1} O_2 range, Merck). The measurement of 5 days Biochemical Oxygen Demand (BOD_5) was performed by means of a mercury-free WTW 2000 Oxytop thermostated at 20 °C. Reactive dyes were analysed using reverse-phase liquid chromatography (flow rate 0.5 mL min^{-1}) and UV–vis detection (543 nm), with a HPLC (Agilent, Series 1100) equipped with a C-18 column (Phenomenex LUNA 5 μm, 3 mm × 150 mm). 5 mmol L^{-1} ammonium acetate (A) and methanol (B) were used as mobile phases. A 15 min gradient elution from 0 to 100% B for Procion Red H-E7B and from 0 to 50% B for Cibacron Red FN-R was used. Ammonium was determined with a Dionex DX-120 ion chromatograph equipped with a Dionex Ionpac CS12A 4 mm × 250 mm column. Isocratic elution was done with a 10 mmol L^{-1} H_2SO_4 solution at 1.2 mL min^{-1}. Anion and carboxylic acid concentrations (in their anionic form) were measured with a Dionex DX-600 ion chromatograph using a Dionex Ionpac AS11-HC 4 mm × 250 mm column. The elution gradient programme for anions involved a 5 min flow with a 20 mmol L^{-1} NaOH solution before the injection, followed by 8 min flow of the same solution after injection, and 7 min with a 35 mmol L^{-1} NaOH solution. The flow rate was 1.5 mL min^{-1}. The gradient programme for carboxylate anions analysis consisted of a 10-min pre-run with a 1 mmol L^{-1} NaOH solution, 10 min with a15 mmol L^{-1} NaOH solution, 10 min with a 30 mmol L^{-1} NaOH solution, and 10 min with a 60 mmol L^{-1} NaOH solution. The flow rate was also 1.5 mL min^{-1}. Iron determination was done by colorimetry (Unicam-2, UV–vis Spectrometer CV2) with 1,10-phenantroline [14]. H_2O_2 consumption was quantified by the potassium iodide titration method [15]. Determination of Total Suspended Solids (TSS) was carried out gravimetrically, following standard methods [14].

2.4. Photo-Fenton experimental set-up

All photo-Fenton experiments were carried out in a solar pilot plant at the PSA (latitude 37°05′N, longitude 2°21′W). The pilot plant (Fig. 2) operated in batch mode and was composed by three CPCs (concentration factor = 1), one tank and one recirculation pump. The collectors (1.03 m^2 each) faced south on a fixed platform tilted 37° (local latitude), and consisted of eight parallel horizontal borosilicate glass-transparent tubes each. Two parabolic aluminium mirrors redirected the radiation toward each tube. Water flowed directly at 20 L min^{-1} from one CPC module to the other and finally into the tank, from where the pump recirculated it back to the CPCs. The total volume (V_T) was 35 L and was separated in two parts: 22 L of total irradiated

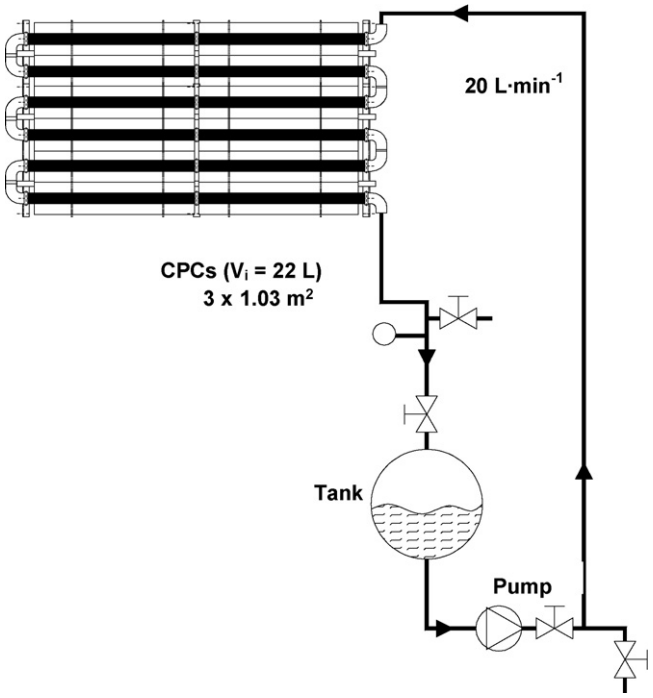

Fig. 2. Scheme of the solar photo-Fenton pilot plant.

volume (V_i) and 13 L of dead reactor volume (tank + connecting tubes) that was not illuminated. More details about the CPC reactor are described elsewhere [16]. Experiments were performed as follows: with the collectors covered, and after pH adjustment around 2.8–3.0, the necessary amounts of iron salt and hydrogen peroxide were added to the tank. After 5 min of homogenisation (dark Fenton reaction), the cover was removed and samples were collected at regular time intervals. Solar ultraviolet radiation (300–400 nm) was measured by a global UV radiometer (Kipp & Zonen, model CUV 3), also tilted 37°, which provided data in terms of incident energy per surface area. In that way, incident radiation could be evaluated as a function of time taking into account cloudiness and other environmental conditions. Thus, experiments could be compared using a corrected illumination time t_{30W} (Eq. (6)) [17],

$$t_{30W,n} = t_{30W,n-1} + \Delta t_n \frac{UV}{30} \cdot \frac{V_i}{V_T}; \quad \Delta t_n = t_n - t_{n-1} \qquad (6)$$

where t_n is the experimental irradiation time for each sample, UV is the average solar ultraviolet radiation measured during Δt_n, and t_{30W} is the "normalised illumination time", i.e., the hypothetic time of constant solar UV power of 30 W m^{-2} (typical solar UV power on a perfect sunny day around noon) needed for the arrival to the collectors of the same energy that is actually received by them along the experimental time t_n. The data corresponding to illumination time can be easily converted into energy input by taking into account that for this photo-reactor the energy delivered when t_{30W} = 4.0 min is 1 kJ L^{-1} [18]. During the present work, UV intensity ranged between 14 and 37 W m^{-2}.

On the other hand, since the system was outdoors, temperature in the reactor changed in the range 25–48 °C. Nevertheless,

comparisons between pilot plant scale data were always done from experiments carried out under similar temperature conditions.

2.5. IBR set-up and operation conditions

The biological pilot plant operated in batch mode and was composed of two independent modules, an IBR and a conditioner tank (50 L). The IBR unit, that consisted of a 35 L column containing plastic supports (polypropylene Pall®-Rings, 15 mm of average diameter), was colonised with activated sludge from a municipal wastewater treatment plant (Almería, Spain). The operational volume was 45 L. A 0.5 L min^{-1} recirculation was maintained between the conditioner tank and the IBR. The system was not thermally controlled and temperature fluctuated between 16 and 40 °C. A blower provided oxygen saturation conditions.

The biological treatment procedure was as follows: once IBR inoculation was carried out, 45 L of a glucose solution (an easily biodegradable substrate) were added to the tank in order to help better growing and fixing of the bacteria on the supports. After complete biodegradation of the glucose, the tank was emptied and sequentially filled with 45 L batches of different photo-treated solutions coming from the photo-Fenton stage. H_2O_2 had been completely consumed before the entry in the IBR (as proven by iodometric titration) and the pH had been previously readjusted from 2.8–3.0 to neutral. The mineralisation of the pre-treated effluent was followed by DOC measurement at regular time intervals (one or two times per day). Other periodical determinations carried out were the evolution of carboxylic acids, NH_4^+, NO_2^- and NO_3^- ions (in order to detect parallel nitrification and denitrification reactions), and TSS, this one to ensure a correct sludge fixation on polypropylene supports (TSS in solution should be close to zero). pH readjustment between 6.5 and 7.5 was done if necessary. Suitable amounts of the following solutions were also supplied to the conditioner tank in order to maintain the required C:N:P (100:20:5) and C:Fe:S (100:2:2) ratios: 43.8 g L^{-1} KH_2PO_4, 27.5 g L^{-1} $CaCl_2$, 22.5 g L^{-1} $MgSO_4{\cdot}7H_2O$, 50 g L^{-1} $FeSO_4{\cdot}7H_2O$, 48 g L^{-1} $NaHCO_3$ and 38.5 g L^{-1} NH_4Cl. The KH_2PO_4, $FeSO_4{\cdot}7H_2O$ and NH_4Cl volumes to be added depended on the DOC present in solution, while the addition of $CaCl_2$ and $MgSO_4{\cdot}7H_2O$ was always fixed in 1 mL L^{-1} of test sample and the addition of $NaHCO_3$ in 2 mL L^{-1} of test sample.

3. Results and discussion

3.1. Preliminary bench-scale degradation of reactive dyes

The application of photo-Fenton reaction either as a single process or as a pre-treatment of an aerobic biological treatment of Procion Red H-E7B and Cibacron Red FN-R was previously done at laboratory scale [10,12,13]. Photo-Fenton oxidation was conducted at 23 °C with a 6 W black light (6 W m^{-2} UVA intensity, measured with a luminometer) situated over a 250 mL photo-reactor (78.54 cm^2 irradiated surface). Biodegradation was carried out under room conditions in a 1.5 L Sequencing Batch Reactor (SBR). The best results for the degradation of an initial 250 mg L^{-1} dye concentration when applying photo-Fenton as a stand-alone process were obtained with 10 mg L^{-1} of Fe (II) and 250 mg L^{-1} of H_2O_2 for Procion Red H-E7B, and 20 mg L^{-1} of Fe (II) and 500 mg L^{-1} H_2O_2 for Cibacron Red FN-R, achieving high degradation levels at short irradiation times: 82 and 84% DOC removal after 100 and 150 min of irradiation, respectively. Those optimal H_2O_2 concentrations closely match the stoichiometrically ones required to completely oxidise the dyes (1 g COD = 0.0312 mol O_2 = 0.0625 mol H_2O_2). On the other hand, in the combined chemical/biological oxidation, 10 mg L^{-1} of Fe (II), and 125 mg L^{-1} of H_2O_2 were needed for 39% mineralisation (60 min) of the homo-bireactive dye, while 20 mg L^{-1} of Fe (II) and 250 mg L^{-1} of H_2O_2 were necessary for 50% mineralisation (90 min) of the hetero-bireactive dye. After those pre-treatment conditions, the coupled SBR system fully mineralised both reactive dyes solutions.

3.2. Photo-Fenton degradation at pilot plant scale

In order to scale-up bench-scale experiments, the same photo-Fenton conditions (10 mg L^{-1} of Fe (II) and 250 mg L^{-1} of H_2O_2 for Procion Red H-E7B, and 20 mg L^{-1} of Fe (II) and 500 mg L^{-1} of H_2O_2 for Cibacron Red FN-R) were initially applied at pilot plant. DOC and H_2O_2 evolution versus t_{30W} is shown in Figs. 3 and 4. As can be observed, a fast mineralisation takes place until the achievement of a constant residual DOC of recalcitrant nature. DOC removal was 82% for Procion Red H-E7B (residual DOC ~ 7 mg L^{-1} C) and 86% for Cibacron Red FN-R (residual DOC ~ 9 mg L^{-1} C), providing evidence of the reproducibility of the laboratory experiments. However, it is noteworthy that the solar photo-Fenton process at the pilot plant involves shorter times of dye degradation than the artificial light process at the laboratory. Maximum mineralisation levels for homo- and hetero-bireactive dyes were attained at t_{30W} = 13 and 22 min, equivalent to 3.3 and 5.0 kJ L^{-1} total energy inputs, respectively. Such results are later discussed in Section 3.4.

3.2.1. Effect of Fe (II) concentration

Initial Fe (II) concentration effect at constant H_2O_2 concentration was evaluated with the base of the photo-Fenton conditions applied at the laboratory. The intention was to determine the lowest amount of iron necessary to effectively carry out the photo-Fenton process in the solar photo-reactor. Therefore, concentrations of Fe (II) lower than 10 mg L^{-1} for Procion Red H-E7B (Fig. 3) and 20 mg L^{-1} for Cibacron Red FN-R (Fig. 4) were evaluated. DOC and H_2O_2 concentration at different t_{30W} were monitored. Overall reaction rate constants could not be calculated because the mineralisation rate did not follow simple kinetic models. This complex behaviour is due to the fact that DOC is the sum of different product concentrations along several simultaneous reactions. Therefore, the t_{30W} necessary to obtain around an 80% mineralisation (defined as $t_{80\%}$) and the maximum slope of the degradation curve (the tangent at the inflexion point, r_0) were chosen to compare the experiments (Table 1). As it can be observed, the higher initial Fe (II) con-

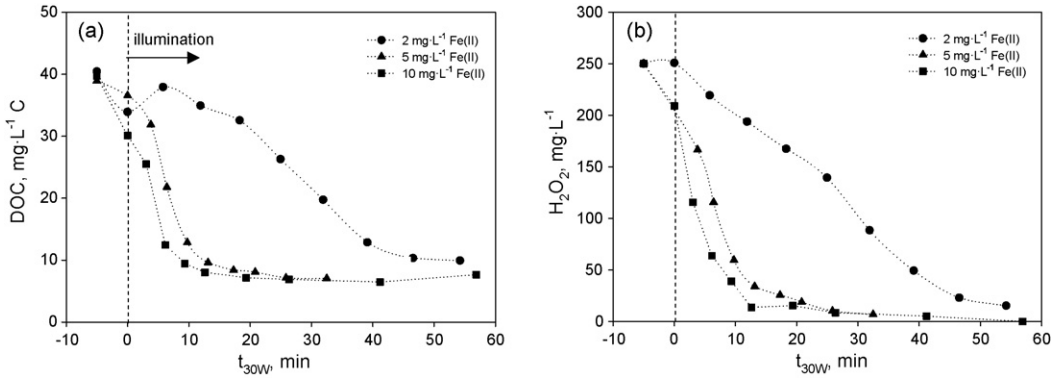

Fig. 3. DOC (a) and H_2O_2 (b) evolution versus t_{30W} at different initial Fe (II) concentrations for 250 mg L^{-1} hydrolysed Procion Red H-E7B degradation; H_2O_2 = 250 mg L^{-1}, pH 2.8.

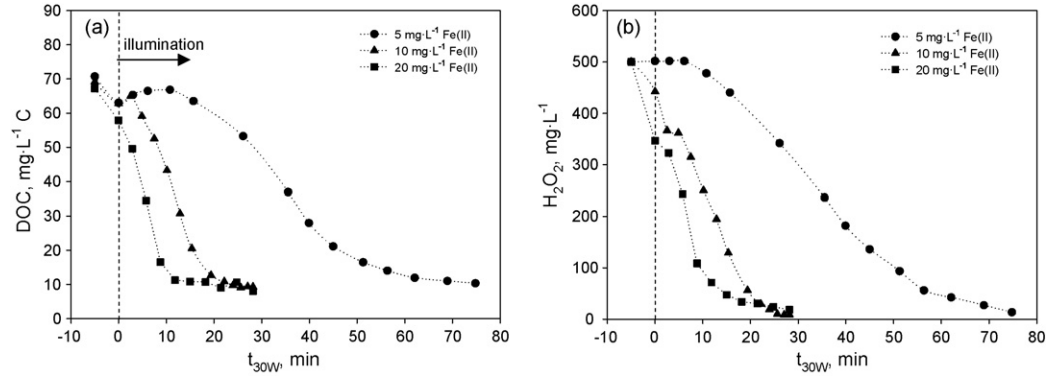

Fig. 4. DOC (a) and H_2O_2 (b) evolution versus t_{30W} at different initial Fe (II) concentrations for 250 mg L^{-1} hydrolysed Cibacron Red FN-R degradation; H_2O_2 = 500 mg L^{-1}, pH 2.8.

centration caused the faster mineralisation, although all tested Fe (II) dosages leaded to the same final degradation level.

Besides, the H_2O_2 concentration presented the same decreasing profile than DOC (Figs. 3 and 4), revealing that both parameters maintained the same correlation regardless of initial Fe (II) concentration. Hence, it can be concluded that 2 and 5 mg L^{-1} were large enough catalyst concentrations to degrade, without losing photo-Fenton efficacy, Procion Red H-E7B and Cibacron Red FN-R, respectively. Those results are interesting from an applied point of view since a low iron concentration would avoid the separation step – based on $Fe(OH)_3$ precipitation – at the end of the oxidation process. Finally, the catalyst evolution (in its total and ferrous form) in relation to t_{30W} is represented in Fig. 5. The fast decrease of Fe (II) concentration in relation to total iron evidences that the rate-limiting step of the catalytic process is the regeneration of ferrous ion from its oxidised form.

The original dye degradation was monitored by HPLC and UV–vis detection. Procion Red H-E7B completely disappeared before illumination (t_{30W} = 0 min) for all Fe (II) concentrations tested, while in the case of Cibacron Red FN-R the 5 mg L^{-1} Fe (II) concentration left part of the dye in solution after the dark Fenton process. The fast dye depletion was accompanied by the solutions decolourisation. Dye concentration decrease versus t_{30W} when using the lowest Fe (II) concentrations is shown in Fig. 6 (no kinetic analysis was possible due to the fast parent

Table 1
Comparison of $t_{80\%}$ and r_0 parameters related to reactive dye degradation for different Fe (II) concentrations

Fe (II)	2 mg L^{-1}		5 mg L^{-1}		10 mg L^{-1}		20 mg L^{-1}	
	$t_{80\%}$ (min)	r_0 (mg L^{-1} min^{-1} C)	$t_{80\%}$ (min)	r_0 (mg L^{-1} min^{-1} C)	$t_{80\%}$ (min)	r_0 (mg L^{-1} min^{-1} C)	$t_{80\%}$ (min)	r_0 (mg L^{-1} min^{-1} C)
Procion Red H-E7B	55	0.49	21	3.88	13	4.20	–	–
Cibacron Red FN-R	–	–	56	0.68	19	2.51	11	5.15

Two hundred and fifty milligrams per liter hydrolysed Procion Red H-E7B, 250 mg L^{-1} H_2O_2; 250 mg L^{-1} hydrolysed Cibacron Red FN-R, 500 mg L^{-1} H_2O_2; pH 2.8.

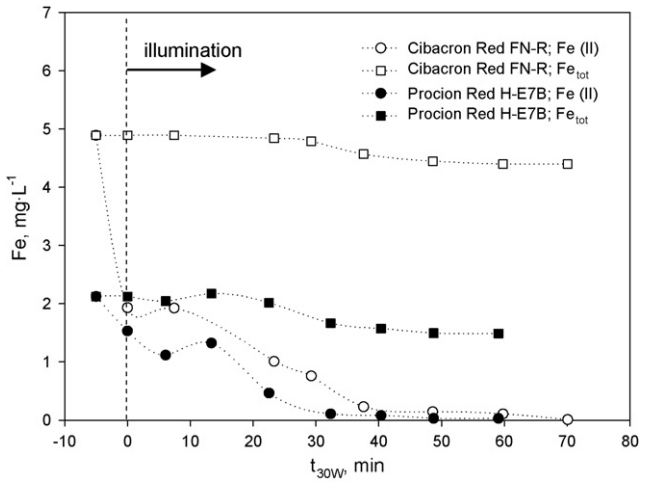

Fig. 5. Fe (II) and total iron evolution versus t_{30W}: 250 mg L^{-1} hydrolysed Procion Red H-E7B, 2 mg L^{-1} Fe (II), 250 mg L^{-1} H_2O_2; 250 mg L^{-1} hydrolysed Cibacron Red FN-R, 5 mg L^{-1} Fe (II), 500 mg L^{-1} H_2O_2; pH 2.8.

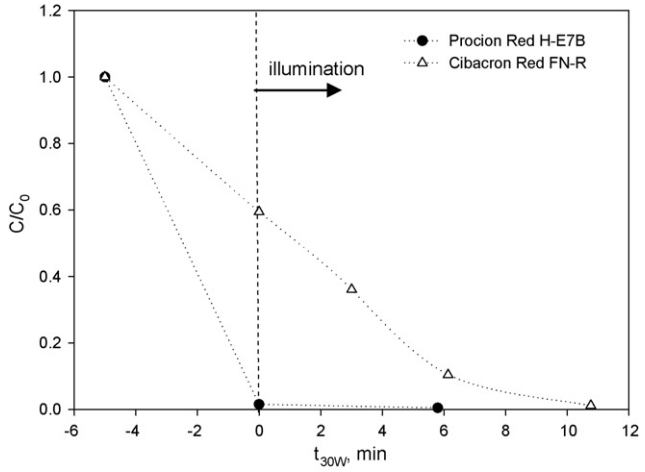

Fig. 6. Relative concentration evolution versus t_{30W}: 250 mg L^{-1} hydrolysed Procion Red H-E7B, 2 mg L^{-1} Fe (II), 250 mg L^{-1} H_2O_2; 250 mg L^{-1} hydrolysed Cibacron Red FN-R, 5 mg L^{-1} Fe (II), 500 mg L^{-1} H_2O_2; pH 2.8.

compound degradation). When comparing reactive dye degradation with mineralisation (Figs. 3(a) and 4(a)), it is noticeable that complete dye disappearance takes place before mineralisation begins. This behaviour seems to suggest a sequenced oxidation mechanism where HO$^{\bullet}$ (of electrophilic nature) preferentially attacks the chromophore centre of the dye molecule (an electron-rich site) [19], giving place to the solution bleaching. Afterwards, mono- or poly-hydroxylations of the aromatic rings would be produced [20,21]. Heteroatoms initially present in the molecule would be released as anions at their highest oxidation states. Finally, a subsequent ring cleavage would generate aliphatic carboxylic acids to finally produce CO_2 and water [22,23].

3.2.2. Carboxylic acids and inorganic compounds generation

Two milligrams per liter of Fe (II) and 250 mg L^{-1} of H_2O_2 for Procion Red H-E7B, and 5 mg L^{-1} of Fe (II) and 500 mg L^{-1} of H_2O_2 for Cibacron Red FN-R were applied in order to determine carboxylic acids and inorganic reaction products. Those low Fe (II) concentrations were used to provide moderate degradation rates that ensure the detection of as many intermediate species as possible. Formic (C_1), acetic (C_2), oxalic (C_2) and maleic (C_4) acids appeared at measurable concentrations during both dyes photo-oxidation. Pyruvic acid (C_3) was also detected during Cibacron Red FN-R photo-treatment (Fig. 7). A significant pH decrease was also observed matching such acids generation. Although they were present in solution from the early stages of the photo-Fenton process, their global concentration reached a maximum around t_{30W} = 30 min for Procion Red H-E7B and between t_{30W} = 13 and 40 min for Cibacron Red FN-R, indicating that they were produced via progressive oxidation of higher molecular weight species. It should be pointed out that, at maximum concentration, the detected carboxylic acids stood for 24% of the total DOC present in solution. Afterwards, their concentration decreased in agreement with the DOC removal until low values or complete disappearance (pH stabilisation) were achieved. 1.1 mg L^{-1} of oxalic acid and 1.5 mg L^{-1} of acetic acid were found at the end of each photo-Fenton process for Cibacron Red FN-R and Procion Red H-E7B, respectively, being the 3 and 9% of the remaining DOC observed (Figs. 3(a) and 4(a)).

As pointed out at the introduction, another important mechanism for the conversion of Fe (III) to Fe (II) is the photo-excitation of the complexes formed between Fe (III) and organic matter, especially carboxylic acids (Eq. (7)). Those

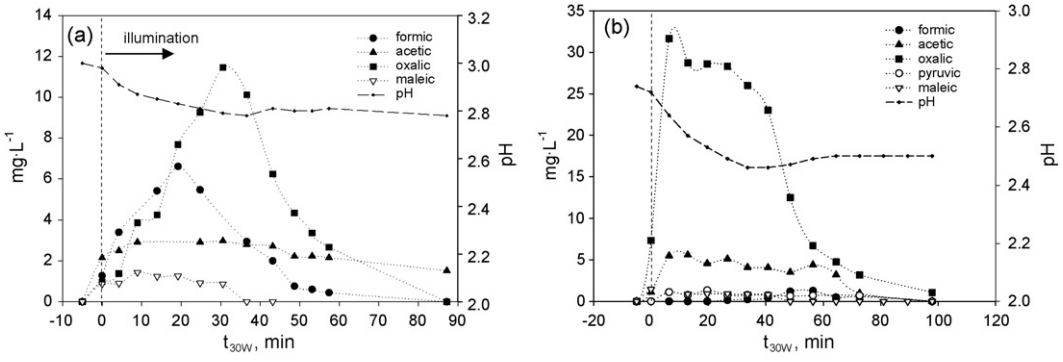

Fig. 7. Carboxylic acids concentration versus t_{30W}. (a) 250 mg L^{-1} hydrolysed Procion Red H-E7B, 2 mg L^{-1} Fe (II), 250 mg L^{-1} H_2O_2; (b) 250 mg L^{-1} hydrolysed Cibacron Red FN-R, 5 mg L^{-1} Fe (II), 500 mg L^{-1} H_2O_2.

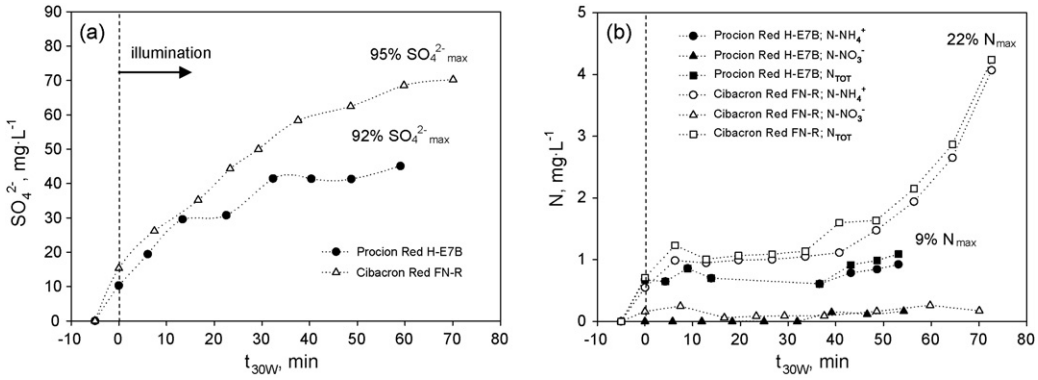

Fig. 8. Sulphate ion (a) and inorganic nitrogen (b) release versus t_{30W}: 250 mg L^{-1} hydrolysed Procion Red H-E7B, 2 mg L^{-1} Fe (II), 250 mg L^{-1} H_2O_2; 250 mg L^{-1} hydrolysed Cibacron Red FN-R, 5 mg L^{-1} Fe (II), 500 mg L^{-1} H_2O_2; pH 2.8.

photochemical reactions, often having larger quantum yields than the excitation of Fe (III) aquo-complexes [7], would lead to an extra fast mineralisation pathway. In agreement with this, it is noticeable that the appearance of the carboxylic acid intermediates, that becomes significant at t_{30W} = 15–20 min of irradiation (Fig. 7), results in an increased DOC removal rate (Figs. 3(a) and 4(a)).

$$[\text{Fe (III) LCOO}]^{2+} \xrightarrow{h\upsilon} \text{Fe (II)} + \text{CO}_2 + \text{L}^{\bullet} \quad (7)$$

Besides DOC removal, dyes mineralisation implies the appearance of inorganic ions. According to the stoichiometric oxidation reactions proposed (Eqs. (8) and (9)), SO_4^{2-} and NO_3^- anions were expected to appear in the media. In order to establish the mass balance of the different elements, and taking into account that the purity of the commercial dyes was unknown, all the initial DOC of the samples was attributed to dye molecules. The difference between the sample carbon weight and the DOC was attributed to inorganic impurities (such as NaCl or Na_2SO_4).

Procion Red H-E7B

$$\text{C}_{52}\text{H}_{34}\text{O}_{26}\text{S}_8\text{Cl}_2\text{N}_{14} + 76.5\text{O}_2 \rightarrow 52\text{CO}_2 + 14\text{NO}_3^- + 8\text{SO}_4^{2-} + 2\text{Cl}^- + 32\text{H}^+ + \text{H}_2\text{O} \quad (8)$$

Cibacron Red FN-R

$$\text{C}_{29}\text{H}_{19}\text{O}_{13}\text{S}_4\text{ClFN}_7 + 41.5\text{O}_2 \rightarrow 29\text{CO}_2 + 7\text{NO}_3^- + 4\text{SO}_4^{2-} + \text{Cl}^- + \text{F}^- + 17\text{H}^+ + \text{H}_2\text{O} \quad (9)$$

The kinetics of appearance of the inorganic anion SO_4^{2-} is presented in Fig. 8(a). Sulphate was gradually released into the solution, in parallel to DOC removal, up to the 92% of the total stoichiometric amount expected for Procion Red H-E7B and the 95% for Cibacron Red FN-R. During the mineralisation process, the –SO_3H group (see Procion Red H-E7B structure, Fig. 1) may be directly substituted by HO$^{\bullet}$ resulting in the release of SO_4^{2-} [24]. The vinylsulphone reactive group of Cibacron Red FN-R (chemical structure not disclosed) would also lead to the sulphate anion formation.

Small nitrate and ammonium concentrations were detected in solution. It is well known that ammonium oxidation by HO$^{\bullet}$ is not a favourable process in acid media, taking place slowly [25]. Fig. 8(b) shows the total nitrogen concentration corresponding to both NH_4^+ and NO_3^- ions generated through the dyes mineralisation. As can be seen, the complete nitrogen mass balance was not obtained, with just 1.1 mg L^{-1} of N for Procion Red H-E7B (9% recovery) and 4.2 mg L^{-1} of N for Cibacron Red FN-R (22% recovery). This incomplete nitrogen mass balance has already been observed in other photocatalytic processes [23,26,27]. Such results seem to be indicative of the presence of N-containing products other than the expected. For instance, taking into account the existence of triazine rings in the studied dyes, a structure difficult to mineralise by photo-Fenton processes [26], it is predictable the presence of triazine derivates in the solution (i.e., ammeline (5N), ammelide (4N) and cyanuric acid (3N)). In this way, only the two N atoms standing outside the triazine ring would be mineralised (the other three N atoms would remain in the triazine ring). The presence of those species could also justify the residual DOC observed at the end of the photo-Fenton process (Figs. 3(a) and 4(a)). For example, in the case of Procion Red H-E7B, the two triazine rings would represent around 65% of the total final DOC. Other studies have reported that nitrogen atoms forming the azo group would lead to N_2 gas generation as a result of the HO$^{\bullet}$ attack [21,22]. More work on degradation products analysis and identification is needed to reveal the complex fate of nitrogen.

3.2.3. Biodegradability enhancement

The biodegradability of Procion Red H-E7B and Cibacron Red FN-R photo-treated solutions, expressed as BOD_5/COD ratio, was determined in order to evaluate photo-Fenton suitability as a previous step of an aerobic biological treatment. 2 mg L^{-1} of Fe (II) for the homo- and 5 mg L^{-1} of Fe (II) for the hetero-bireactive dye were used to carry out the oxidation. As pointed out above, the lowest iron concentration was used to avoid the need for Fe separation at the end of the chemical oxidation, before the biological process. Hydrogen peroxide was gradually added to determine the minimum concentration able to generate a bio-compatible effluent. Each new H_2O_2 pulse

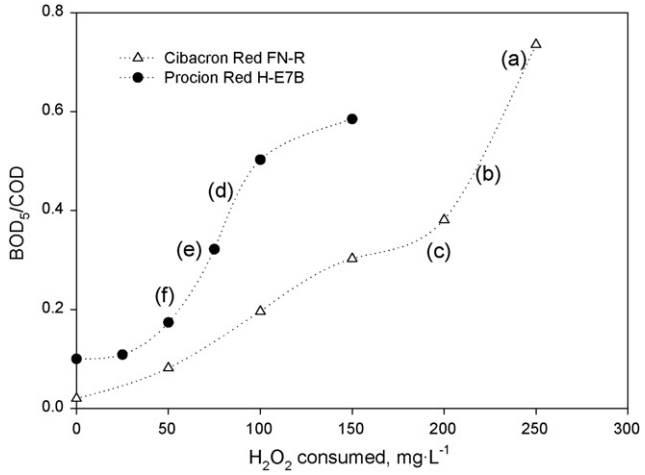

Fig. 9. BOD_5/COD evolution versus H_2O_2 consumption for 250 mg L^{-1} hydrolysed Procion Red H-E7B (2 mg L^{-1} Fe (II)) and 250 mg L^{-1} hydrolysed Cibacron Red FN-R (5 mg L^{-1} Fe (II)); pH 2.8.

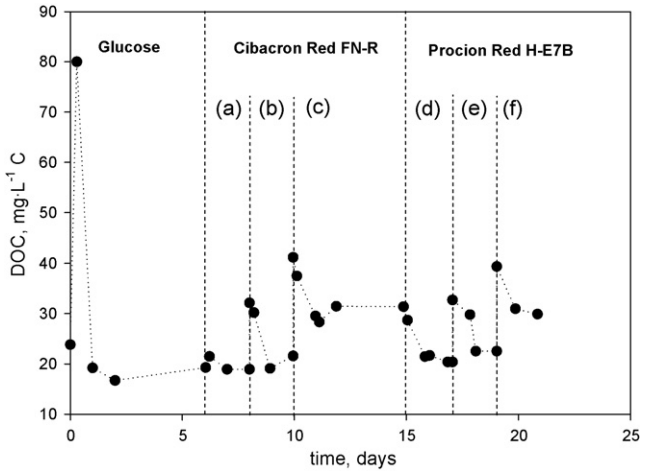

Fig. 10. IBR operation after photo-Fenton pre-treatment: 250 mg L^{-1} hydrolysed Cibacron Red FN-R, 5 mg L^{-1} Fe (II), (a) 250 mg L^{-1} H_2O_2, (b) 225 mg L^{-1} H_2O_2, (c) 200 mg L^{-1} H_2O_2; 250 mg L^{-1} hydrolysed Procion Red H-E7B, 2 mg L^{-1} Fe (II), (d) 80 mg L^{-1} H_2O_2, (e) 65 mg L^{-1} H_2O_2 and (f) 50 mg L^{-1} H_2O_2.

was added after complete H_2O_2 consumption. BOD_5/COD ratio versus H_2O_2 added is represented in Fig. 9. As can be seen biodegradable solutions can be obtained with increasing H_2O_2 amounts, easily attaining the $BOD_5/COD = 0.4$ value characteristic of thoroughly biodegradable wastewaters [28].

3.3. Immobilised Biomass Reactor

Cibacron Red FN-R and Procion Red H-E7B photo-treated solutions were used to feed the IBR pilot plant. As it has been described in Section 2, a batch of glucose (DOC around 80 mg L^{-1} C) was previously added to the conditioner tank to ensure the biomass viability. This also let to establish the lower residual DOC that could be achieved by the IBR system (~20 mg L^{-1} C) due to the unavoidable presence of biomass metabolites. Afterwards, a pre-designed sequence was followed to fill the reactor with the photo-treated samples. For Cibacron Red FN-R solutions (5 mg L^{-1} of Fe (II)): (a) 250 mg L^{-1} of H_2O_2 (DOC = 24 mg L^{-1} C); (b) 225 mg L^{-1} of H_2O_2 (DOC = 34 mg L^{-1} C); (c) 200 mg L^{-1} of H_2O_2 (DOC = 42 mg L^{-1} C). For Procion Red H-E7B solutions (2 mg L^{-1} of Fe (II)): (d) 80 mg L^{-1} of H_2O_2 (DOC = 29 mg L^{-1} C); (e) 65 mg L^{-1} of H_2O_2 (DOC = 33 mg L^{-1} C); (f) 50 mg L^{-1} of H_2O_2 (DOC = 39 mg L^{-1} C). The treatment started with the more biodegradable samples (larger H_2O_2 concentration used) changing later to the ones with a lower BOD_5/COD ratio, trying to find out the minimum H_2O_2 dose needed for a successful and complete chemical/biological treatment. Proceeding in that way, bacteria were able to get used to the photo-treated wastewater. Full biodegradation was assumed when attaining residual DOC values close to those obtained in the previous glucose batch (~20 mg L^{-1} C).

From Fig. 10, it is clear that Cibacron Red FN-R solution was completely biodegraded in 1–2 days when adding 250 and 225 mg L^{-1} of H_2O_2 (doses a and b) in the photo-Fenton stage. However, the IBR was not able to degrade the hetero-bireactive dye by-products generated when using only 200 mg L^{-1} of H_2O_2 (c). The same behaviour was observed for Procion Red H-E7B. The effluents resulting when using 80 and 65 mg L^{-1} of H_2O_2 (doses d and e) were fully biodegraded while the one using 50 mg L^{-1} of H_2O_2 (f) was not bio-compatible enough to feed the biological pilot plant. HPLC analysis revealed that the original dyes were not present in solution at the end of each photo-treatment. This fact indicates that the non-biodegradability of (c) and (f) solutions was due to the presence of dyestuff by-products of bio-recalcitrant nature. Finally, it is remarkable that maximum concentrations of compounds of biodegradable nature like aliphatic carboxylic acids (around 24% of the total DOC, see Section 3.2.2) were detected in the bio-compatible effluents (a, b, d and e). Regarding inorganic compounds generation, solutions became biodegradable after 63 and 79% desulphuration and after 6 and 9% N release for Procion Red H-E7B and Cibacron Red FN-R, respectively. The differences between the photo-Fenton conditions tested are shown in Fig. 11 where the percentages of mineralisation reached in each stage of the coupling are compared. The residual DOC values oscillated around 20 mg L^{-1} C, in accordance with the lower threshold for DOC removal.

Nitrification and denitrification reactions were followed up by NH_4^+, NO_2^- and NO_3^- ion concentration measurements. A complete nitrification was achieved at the end of each batch biodegradation, indicating that the IBR system was working properly. Moreover, aliphatic carboxylic acids initially present in the pre-treated effluents were completely removed from the solutions.

The above results show that, as happens when working under laboratory conditions, the photo-Fenton reaction can be successfully used as a pre-treatment to make biodegradable the original reactive dye solutions. Among the tested pre-treatment conditions, the best ones for a subsequent biodegradation at pilot plant are 5 mg L^{-1} of Fe (II) and 225 mg L^{-1} of H_2O_2 for Cibacron Red FN-R and 2 mg L^{-1} of Fe (II) and 65 mg L^{-1}

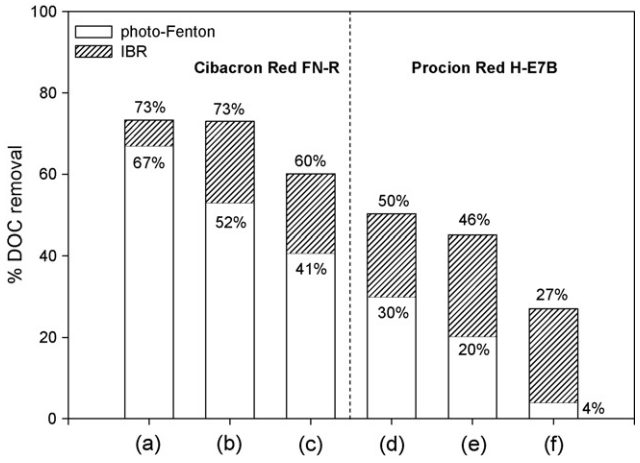

Fig. 11. % DOC removal in photo-Fenton pre-treatment and IBR coupling system as a function of photo-Fenton conditions: 250 mg L^{-1} hydrolysed Cibacron Red FN-R, 5 mg L^{-1} Fe (II), (a) 250 mg L^{-1} H_2O_2, (b) 225 mg L^{-1} H_2O_2, (c) 200 mg L^{-1} H_2O_2; 250 mg L^{-1} hydrolysed Procion Red H-E7B, 2 mg L^{-1} Fe (II), (d) 80 mg L^{-1} H_2O_2, (e) 65 mg L^{-1} H_2O_2 and (f) 50 mg L^{-1} H_2O_2.

of H_2O_2 for Procion Red H-E7B. BOD_5/COD values around 0.4 were achieved (Fig. 9), with 52 and 20% mineralisation levels, respectively.

3.4. Main differences between laboratory and pilot plant

There are some fundamental differences between the photo-Fenton experiments carried out in the laboratory and in the pilot plant. First of all, the source of irradiation and the temperature were significantly different. A 6 W black light, a lamp that only emits photons in the UVA range, was used in the laboratory, while the pilot plant reactor was irradiated by the complete sunlight spectrum at the earth surface. Taking the 30 W m^{-2} value as an estimation of the 300–400 nm energy arriving to the earth surface around noon, the energy entering the photo-reactor from the artificial black light was five times lower. Additionally, it should be noted that the PSA radiometer measured only the 300–400 nm bandwidth of the solar spectrum, while photo-Fenton reaction also makes use of part of the visible spectrum [8]. This fact favours the pilot plant results and complicates the comparison with laboratory experiments. The high levels of temperature reached during solar photo-Fenton experimentation (from 25 up to 48 °C) also involve a general increase of dye removal rates due to the beneficial effect of temperature on Fenton reaction [29].

Photo-reactors were also different from one system to the other, leading to different efficiencies with regard to radiation absorption. At the laboratory, with the artificial light over the batch reactor, all solution volume was under irradiation, but the depth and the aromatic content of solutions caused a strong absorption and impeded the radiation penetration towards the bottom of the system. On the contrary, the CPC configuration allowed all the illuminated volume to receive photons since solar light entered the solution through all the circumference of the reactor tubes.

As observed before, mineralisation yields were closely reproduced when scaling-up from laboratory to pilot plant the 10 mg L^{-1} of Fe (II) and 250 mg L^{-1} of H_2O_2 photo-Fenton conditions for Procion Red H-E7B and the 20 mg L^{-1} of Fe (II) and 500 mg L^{-1} of H_2O_2 for Cibacron Red FN-R. The reduction of irradiation times (from 100 and 150 min of black light irradiation to t_{30W} = 13 and 22 min, respectively) was a direct consequence of the above-explained factors. This fast reaction rate allowed the pilot plant to reduce the catalyst concentration from 10 to 2 mg L^{-1} for Procion Red H-E7B and from 20 to 5 mg L^{-1} for Cibacron Red FN-R without loosing mineralisation yields (see Figs. 3 and 4). Besides the reaction times, laboratory and pilot plant results may also be compared in terms of energy inputs. At laboratory scale, a simple calculation taking into account the energy reaching the reactor (W m^{-2}), the irradiation time required to attain the 82–84% mineralisation, the reactor volume, as well as the reactor irradiated surface, gives an accumulated energy input of 1.1 and 1.7 kJ L^{-1} for Procion Red H-E7B and Cibacron Red FN-R, respectively. Those values are significantly lower than the 3.3 and 5.0 kJ L^{-1} obtained at pilot plant. Obviously, the apparent photonic efficiency of the process (defined as photogenerated reaction rate versus volumetric light intensity entering the reactors) is not the same for both configurations. Although the solar pilot plant is more efficient in terms of reaction time, it is less efficient in terms of energy consumption since more photons are needed in order to provide the same final dye mineralisation. In the combined chemical/biological treatment at pilot plant, pre-treatment conditions similar to those used at the laboratory were necessary to obtain a completely biodegradable Cibacron Red FN-R solution. The best results were obtained with 250 mg L^{-1} of H_2O_2 at the laboratory and 225 mg L^{-1} of H_2O_2 at pilot plant, leading to 50 and 52% mineralisation, respectively. However, for Procion Red H-E7B dye degradation, photo-Fenton oxidation at pilot plant improved laboratory results reducing the H_2O_2 requirements from 125 to 65 mg L^{-1}, and the mineralisation yield from 39 to 20%.

4. Conclusions

The solar pilot plant photo-Fenton processes for Procion Red H-E7B and Cibacron Red FN-R reactive dyes mineralisation closely reproduced previous laboratory artificial light results. 82 and 86% mineralisation were accomplished by adding 10 mg L^{-1} of Fe (II) and 250 mg L^{-1} of H_2O_2 to 250 mg L^{-1} of Procion Red H-E7B solutions, and 20 mg L^{-1} of Fe (II) and 500 mg L^{-1} of H_2O_2 to 250 mg L^{-1} of Cibacron Red FN-R solutions, respectively.

The irradiation time was reduced in relation to the artificial light process from 100 and 150 min (black light irradiation) to 13 and 22 min (normalised t_{30W} values), basically due to the higher amount of UV photons supplied by the sun, the involvement of the visible fraction of sunlight spectrum, and the solar photoreactor configuration, which collects and redirects to the solution all the radiation reaching the aperture area of the CPCs. Nevertheless, with the high photon flux of the pilot plant the apparent photonic efficiency of the process decreases. The fast reaction

rates allowed the pilot system to reduce the use of iron from 10 to 2 mg L^{-1} for Procion Red H-E7B and from 20 to 5 mg L^{-1} for Cibacron Red FN-R without loosing photo-Fenton yields.

Formic, acetic, oxalic and maleic acids appeared during both dyes photo-oxidations. Pyruvic acid was also a detected intermediate for Cibacron Red FN-R dye. Sulphur was stoichiometrically released into the solution as sulphate ion, with 92–95% recovery. The nitrogen mass balance was not completed since only 9–22% of the total N was detected as inorganic nitrogen (NH_4^+ and NO_3^-) at the end of the treatment. Those results are indicative of the generation of other N-containing products, such as N_2 gas and the recalcitrant triazine ring.

Finally, solar photo-Fenton process at pilot plant can be successfully used as a biological pre-treatment. With just 5 mg L^{-1} of Fe (II) and 225 mg L^{-1} of H_2O_2 (Cibacron Red FN-R) and 2 mg L^{-1} of Fe (II) and 65 mg L^{-1} of H_2O_2 (Procion Red H-E7B), dye solutions became enough bio-compatible to be fully biodegraded in the IBR reactor, attaining residual DOC values close to the 20 mg L^{-1} of C corresponding to biomass metabolites. In comparison with bench-scale experiments, the performance of the pilot plant combined chemical/biological treatment appears to be superior.

Acknowledgements

The authors wish to thank to the Ministerio de Educación y Ciencia (project CTQ 2005-02808) for financial support and the "Programa de Acceso y Mejora de Grandes Instalaciones Científicas Españolas" (project GIC-05-17).

References

[1] C. O'Neill, F.R. Hawkes, D.L. Hawkes, N.D. Lourenço, H.M. Pinheiro, W. Delée, J. Chem. Technol. Biotechnol. 74 (11) (1999) 1009–1018.
[2] R. Andreozzi, V. Caprio, A. Insola, R. Marotta, Catal. Today 53 (1999) 51–59.
[3] R. Bauer, H. Fallman, Res. Chem. Intermed. 23 (1997) 341–354.
[4] J. Pignatello, Environ. Sci. Technol. 26 (1992) 944–951.
[5] A. Safarzadeh-Amiri, J.R. Bolton, S.R. Cater, J. Adv. Oxid. Technol. 1 (1996) 18–26.
[6] J. Pignatello, D. Liu, P. Huston, Environ. Sci. Technol. 33 (1999) 1832–1839.
[7] K.A. Hislop, J.R. Bolton, Environ. Sci. Technol. 33 (1999) 3119–3126.
[8] R. Bauer, G. Waldner, H. Fallmann, S. Hager, M. Klare, T. Krutzler, S. Malato, P. Maletzky, Catal. Today 53 (1999) 131–144.
[9] M.J. Farré, X. Domènech, J. Peral, Water Res. 40 (2006) 2533–2540.
[10] J. García-Montaño, F. Torrades, J.A. García-Hortal, X. Domènech, J. Peral, Appl. Catal. B: Environ. 67 (2006) 86–92.
[11] V. Sarria, S. Kenfack, O. Guillod, C. Pulgarín, J. Photochem. Photobiol. A 159 (2003) 89–99.
[12] J. García-Montaño, F. Torrades, J.A. García-Hortal, X. Domènech, J. Peral, J. Hazard. Mater. 134 (2006) 220–229.
[13] F. Torrades, J. García-Montaño, J.A. García-Hortal, Ll. Núñez, X. Domènech, J. Peral, Color. Technol. 120 (2004) 188–194.
[14] APHA-AWWA-WEF, Standard Methods for the Examination of Water and Wastewater, eighteenth ed., Washington, DC, 1992.
[15] C. Kormann, D.W. Bahnemann, M.R. Hoffmann, Environ. Sci. Technol. 22 (5) (1988) 798–806.
[16] J. Blanco, S. Malato, P. Fernández, A. Vidal, A. Morales, P. Trincado, J.C. Oliveira, C. Minero, M. Musci, C. Casalle, M. Brunote, S. Tratzky, N. Dischinger, K.-H. Funken, C. Sattler, M. Vincent, M. Collares-Pereira, J.F. Mendes, C.M. Rangel, Sol. Energy 67 (2000) 317–330.
[17] S. Malato, J. Cáceres, A.R. Fernández-Alba, L. Piedra, M.D. Hernando, A. Agüera, J. Vial, Environ. Sci. Technol. 37 (2003) 2516–2524.
[18] S. Malato, J. Cáceres, A. Agüera, M. Mezcua, D. Hernando, J. Vidal, A.R. Fernández-Alba, Environ. Sci. Technol. 35 (2001) 4359–4366.
[19] C. Galindo, P. Jacques, A. Kalt, J. Photochem. Photobiol. A 130 (2000) 35–47.
[20] E. Guivarch, S. Trevin, C. Lahitte, M.A. Oturan, Environ. Chem. Lett. 1 (2003) 38–44.
[21] C. Hu, J.C. Yu, Z. Hao, P.K. Wong, Appl. Catal. B: Environ. 42 (2003) 47–55.
[22] M. Karkmaz, E. Puzenat, C. Guillard, J.M. Herrmann, Appl. Catal. B: Environ. 51 (2004) 183–194.
[23] M. Stylidi, D.I. Kondarides, X.E. Verykios, Appl. Catal. B: Environ. 40 (2003) 271–286.
[24] H. Lachheb, E. Puzenat, A. Houas, M. Ksibi, E. Elaloui, C. Guillard, J.M. Herrmann, Appl. Catal. B: Environ. 39 (2002) 75–90.
[25] A. Bravo, J. García, X. Domènech, J. Peral, J. Chem. Res. S (1993) 376–377.
[26] M.H. Pérez, G. Peñuela, M.I. Maldonado, O. Malato, P. Fernández-Ibáñez, I. Oller, W. Gernjak, S. Malato, Appl. Catal. B: Environ. 64 (2006) 272–281.
[27] M. Lapertot, C. Pulgarín, P. Fernández-Ibáñez, M.I. Maldonado, L. Pérez-Estrada, I. Oller, W. Gernjak, S. Malato, Water Res. 40 (2006) 1086–1094.
[28] E. Chamarro, A. Marco, S. Esplugas, Water Res. 35 (2001) 1047–1051.
[29] M. Pérez, F. Torrades, X. Domènech, J. Peral, Water Res. 36 (2002) 2703–2710.